The Phleboviruses Sandfly Fever Naples Virus and Toscana Virus Uncouple the Rnase and Kinase Activity of IRE1

Francesca Palma, Carla Zannella, Rosa Giugliano, Anna Riccio, Simone La Frazia, Valentina Svicher, Anna De Filippis, Massimiliano Galdiero

Affiliations

[1]Department of Women, Children and General And Specialized Surgery, University of Campania "Luigi Vanvitelli", 80138 Naples, Italy;
[2]Department of Biology, University of Roma "Tor Vergata", 00133, Rome, Italy;
[3]Complex Operative Unit of Virology and Microbiology, University Hospital of Campania "Luigi Vanvitelli", 80138 Naples.

Background

Toscana virus (TOSV) and Sandfly Fever Naples virus (SFNV) are the most common phleboviruses in the Mediterranean Basin. Although antigenically related, they differ in pathogenicity: TOSV exhibits pronounced neurotropism and can cause severe or fatal neurological disease, whereas SFNV typically induces a transient, self-limiting, flu-like illness. No vaccine or specific antivirals are currently available against phleboviral infections. Understanding their replication cycles and interactions with host defenses is therefore essential. One of the earliest cellular defense mechanisms is the unfolded protein response (UPR), triggered by endoplasmic reticulum (ER) stress and capable of inducing autophagy or apoptosis. Conversely, viruses exploit host translation and often manipulate the UPR to enhance replication. This study investigates how TOSV and SFNV modulate UPR signaling during infection, and the cell fate induced by ER stress. Our results provide new insights into virus–host interactions and identify potential targets for therapeutic intervention.

Materials and Methods

Human lung carcinoma (A549) cells were infected with TOSV and SFNV (MOI=3) and monitored over a 16-hour time course for RNA and protein extraction. The expression of key UPR effectors (BiP/Grp78, PERK, ATF6, IRE1, ATF4, CHOP, and eIF2α) was analysed by quantitative PCR and Western Blotting. Unspliced and spliced XBP1 transcripts were detected by PCR to assess IRE1 pathway activation. The two IRE1-induced cell fates (apoptosis and autophagy) were evaluated via Western Blot Furthermore, the impact of pharmacological modulation of UPR and autophagy flux on viral replication was assessed by determining viral yields in the presence of selected modulators.

Results

The active (=phosphorylated) form of IRE1 was strongly upregulated during the late phase of infection (9-16 hours post-infection). Notably, the spliced form of XBP1 was not detected, suggesting that either virus may interfere with IRE1 RNase activity. Therefore, the kinase activity of IRE1 was assessed by measuring its downstream effects on cell fates: apoptosis and autophagy. PARP serving as an apoptotic marker, was found to be in its full form, indicating that the apoptotic process didn't occur. By contrast, JNK, p62 and LC3 served as autophagic hallmarks. Interestingly, aligning with IRE1 activation pattern, phospho-JNK was found as early as 9 hours post-infection, for both viruses. In the meantime, p62 decreased over time and the lipidated form of LC3 (LC3-II) increased, both starting at 13.5 hours post-infection, indicating an active autophagic flux upon SFNV and TOSV infection.

Treatments with chemical modulators of UPR (4-PBA), IRE1 (KIRA6 and STF083010), PERK (GSK2656157), autophagosome-lysosome fusion (CQ), and autophagolysosome acidification (BafA1), confirmed that the IRE1-JNK-autophagy signaling cascade is beneficial to the SFNV and TOSV life cycle.

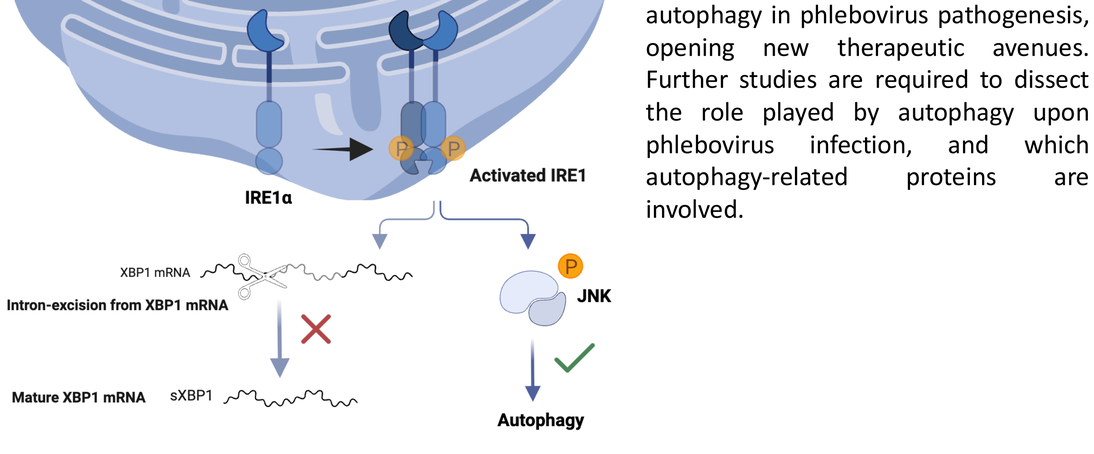

Fig 6. Pharmacological modulation of the UPR-JNK-autophagy axis and its effects on SFNV and TOSV replication. The biological relevance between pharmacological treatments and the absence of treatment (set as 0 in the analysis, and reported as dashed line at y=0 in the graph) was assessed with one-way ANOVA, with Dunnett's multiple comparisons test as post-hoc analysis (p-value < 0.0215 ** p-value < 0.0079, *** p-value = 0.0001).*

Conclusions

These findings reveal a previously unrecognized role for the UPR and autophagy in phlebovirus pathogenesis, opening new therapeutic avenues. Further studies are required to dissect the role played by autophagy upon phlebovirus infection, and which autophagy-related proteins are involved.

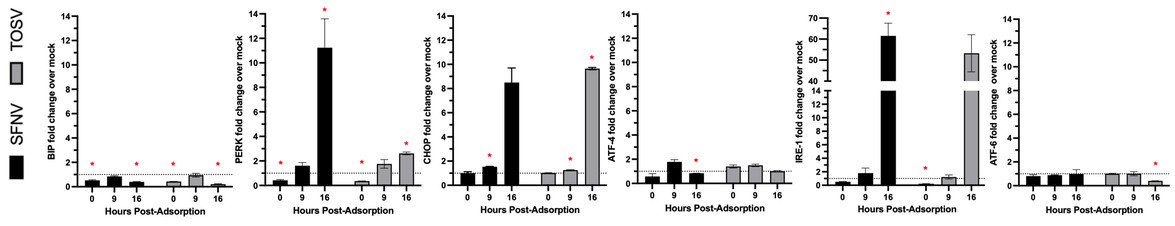

Fig 1. Preliminary assessment of viral impact on key UPR effectors expression, evaluated by qPCR at three different times post-adsorption (0-9-16 hpa). The data are presented as mean ± SD. Statistical significance was calculated using a two-tailed, paired t-test (p < 0.05).*

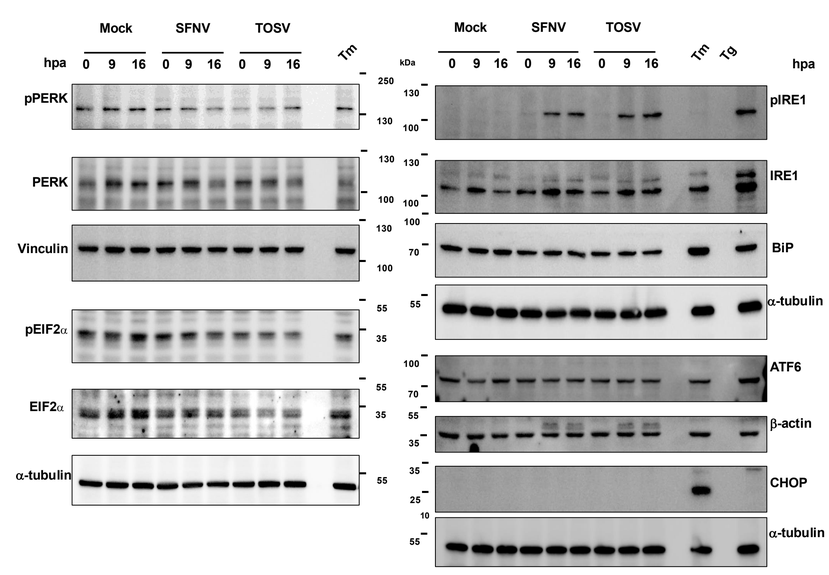

Fig 2. The UPR branch of IRE1 is activated by SFNV and TOSV infection. Total cellular protein content was harvested at the indicated time points and probed against selected antibodies. The loading controls (vinculin, α-tubulin, or β-actin) were chosen according to the molecular weight of the target protein. Representative blot images are shown.

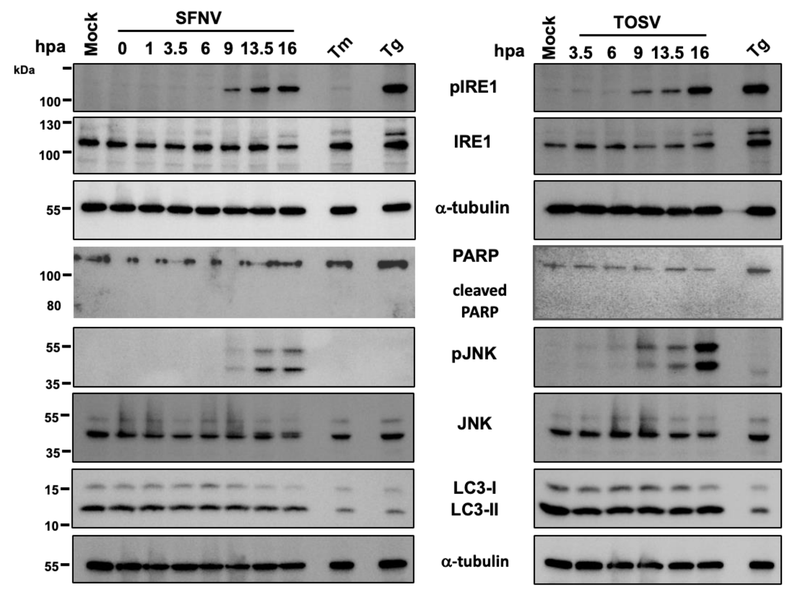

Fig 3. SFNV and TOSV activate the IRE1-JNK-autophagy axis at late infection phases. IRE1 is phosphorylated and active from 9 hpa until the end of the course of infection. One of its downstream targets, JNK, was found phosphorylated at 13.5 and 16 hpa, as well. The conversion from the cytosolic form of LC3 (LC3-I) to its lipidated one (LC3-II), was used as an autophagic marker, and checked. According to the phosphorylated status of JNK, the lipidated LC3 was readily detected at 13.5 and 16 hpa, confirming the occurrence of the autophagic process at later stages of infection. PARP was used to detect apoptosis occurrence. Tunicamycin (Tg, 5 μg/mL) and Thapsigargin (Tg, 1 μM) served as positive controls for UPR.

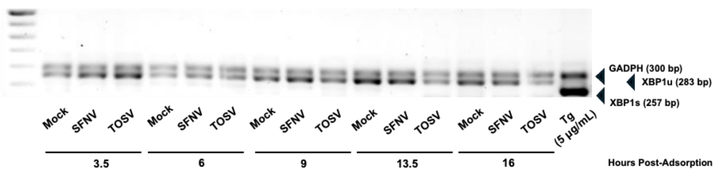

Fig 4. XBP1 splicing detection by PCR during the time range 3.5 - 16 hpa for SFNV-, TOSV-, and mock-infected A549. XBP1 full form (uXBP1) is 283 base pairs (bp) long; if IRE1 excises from the XBP1 transcript 26 nucleotides (nt), the resulting band is 257 bp (sXBP1). Tg (5 μg/mL for 9 h) constituted the positive control, while GAPDH (with an amplification band of 300 bp) served as loading control.

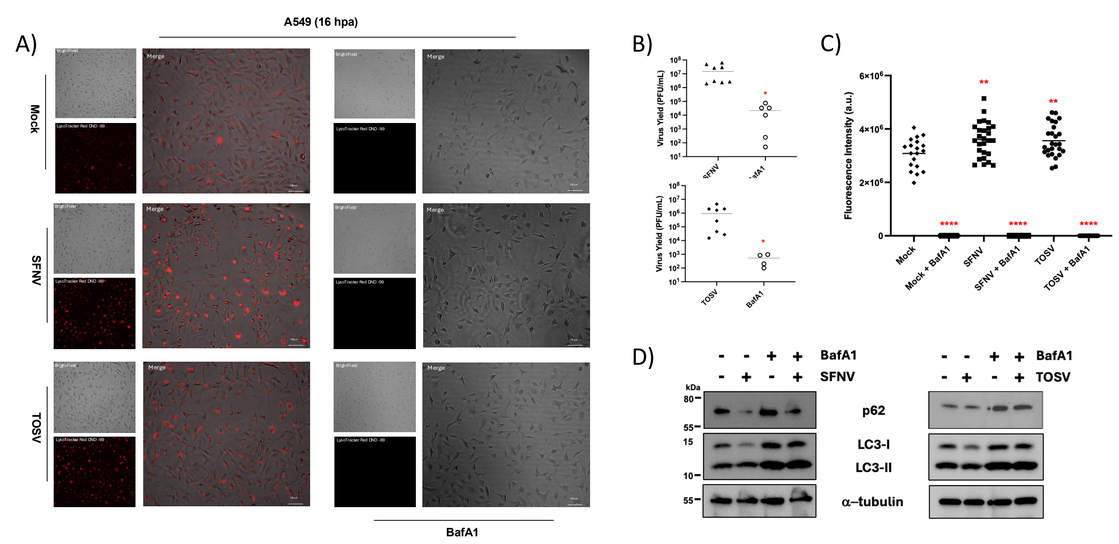

*Fig 5. SFNV and TOSV positively modulate autophagy flux. A) A549 cells were infected with either SFNV or TOSV. BafA1-treated (infected and uninfected) counterpart served as control. Acidic lysosomes, used as autophagic marker, were stained with LysoTracker Red DND-99 for 30 min at standard conditions. All images were acquired with a Nikon Eclipse Ti-2U fluorescence microscope, under the same conditions. Scale bar: 100 μm. (B) The viral yield from infected- and infected-BafA1 treated- cells, were quantified by titration on Vero-76 and crystal violet staining. Student's t-test was used to evaluate the statistical relevance between the BafA1-treated and untreated virus. * p < 0.05. (C) Fluorescence intensity from acidic lysosomes was measured using ImageJ software. One-way ANOVA (with Dunnett's multiple comparisons test) provided the statistical significance of the fluorescence intensity changes between the mock-infected, virus-infected and BafA1-treated, SFNV/TOSV-infected, and SFNV/TOSV-infected and BafA1-treated cells (** p < 0.0082, **** p < 0.0001). D) BafA1 treatment rescued the LC3-I and p62 levels in infected cells, indicating an incomplete autophagic flux which negatively correlated with viral replication.*

Let's stay in touch
francesca.palma@unicampania.it

viruses
MDPI
Viruses 2026 Conference